Published in "Paleoceanography 31(3): 2015PA002859, 2016"
which should be cited to refer to this work.

Paleoseawater density reconstruction and its implication for cold-water coral carbonate mounds in the northeast Atlantic through time

Andres Rüggeberg[1,2,3], Sascha Flögel[2], Wolf-Christian Dullo[2], Jacek Raddatz[2,4], and Volker Liebetrau[2]

[1]Unit of Earth Sciences, Department of Geosciences, University of Fribourg, Fribourg, Switzerland, [2]GEOMAR Helmholtz Centre for Ocean Research Kiel, Kiel, Germany, [3]Renard Centre of Marine Geology, Ghent University, Gent, Belgium, [4]Now at Institute of Geosciences, Goethe University Frankfurt, Frankfurt am Main, Germany

Key Points:
- Regional seawater density reconstruction for the NE Atlantic during the Pleistocene
- Cold-water coral carbonate mounds in relation to seawater density during the Pleistocene
- Importance of intermediate water mass dynamics on cold-water coral ecosystems

Supporting Information:
- Supporting Information S1

Correspondence to:
A. Rüggeberg,
andres.rueggeberg@unifr.ch

Abstract Carbonate buildups and mounds are impressive biogenic structures throughout Earth history. In the recent NE Atlantic, cold-water coral (CWC) reefs form giant carbonate mounds of up to 300 m of elevation. The expansion of these coral carbonate mounds is paced by climatic changes during the past 2.7 Myr. Environmental control on their development is directly linked to controls on its main constructors, the reef-building CWCs. Seawater density has been identified as one of the main controlling parameter of CWC growth in the NE Atlantic. One possibility is the formation of a pycnocline above the carbonate mounds, which is increasing the hydrodynamic regime, supporting elevated food supply, and possibly facilitating the distribution of coral larvae. The potential to reconstruct past seawater densities from stable oxygen isotopes of benthic foraminifera has been further developed: a regional equation gives reliable results for three different settings, *peak interglacials* (e.g., Holocene), *peak glacials* (e.g., Last Glacial Maximum), and *intermediate* setting (between the two extremes). Seawater densities are reconstructed for two different NE Atlantic CWC carbonate mounds in the Porcupine Seabight indicating that the development of carbonate mounds is predominantly found at a seawater density range between 27.3 and 27.7 kg m^{-3} (σ_Θ notation). Comparable to recent conditions, we interpret the reconstructed density range as a pycnocline serving as boundary layer, on which currents develop, carrying nutrition and possibly coral larvae. The close correlation of CWC reef growth with reconstructed seawater densities through the Pleistocene highlights the importance of pycnoclines and intermediate water mass dynamics.

1. Introduction

Cold-water coral (CWC) reefs are spectacular marine ecosystems [e.g., *Freiwald et al.*, 2004], promoting high biodiversity and a high density of marine life almost comparable to shallow-marine tropical reefs. These prominent systems are under varying degrees of pressure due to bottom trawling, hydrocarbon extraction, deep-sea mining and bio prospecting, bottom water warming, and ocean acidification [*European Commission*, 2007; *Intergovernmental Panel on Climate Change*, 2014]. The European continental margin is known for its high density of CWC reefs [*Roberts et al.*, 2006]. In the Porcupine Seabight along the margin off SW Ireland these CWC reefs form carbonate mounds, which occur in distinct provinces [*Henriet et al.*, 1998; *Dorschel et al.*, 2010] (Figure 1). IODP Expedition 307 drilled through Challenger Mound and indicates earliest CWC growth at 2.5–2.7 million years ago (Ma) [*Kano et al.*, 2007], while later studies assume a slightly earlier initiation between 2.7 Ma and 3 Ma [*Foubert and Henriet*, 2009; *Raddatz et al.*, 2011, 2014; *Thierens et al.*, 2013].

The geographical distribution and sustained development of CWC reefs have proven to be strongly related to climate influences over the past three glacial-interglacial cycles [*Frank et al.*, 2011]. More important for the carbonate mounds, the formation of CWC reefs strongly relies on the sediment baffling capacity of their major frame builders, the azooxanthellate cold-water corals *Lophelia pertusa* and *Madrepora oculata*. Further physical and chemical parameters like temperature, nutrition, currents, and the existence of a well-expressed pycnocline (density gradient) have been identified as important drivers of environmental control for these CWC ecosystems during past glacial-interglacial times [e.g., *Dorschel et al.*, 2005; *Roberts et al.*, 2006; *Rüggeberg et al.*, 2007; *Wienberg et al.*, 2010]. More recently, different studies report of the possible significance of seawater carbonate parameters like dissolved inorganic carbon, pH, total alkalinity, aragonite saturation ($\Omega_{aragonite}$), pCO_2, [HCO_3^-], and [CO_3^{2-}] on the growth of different CWC species and their

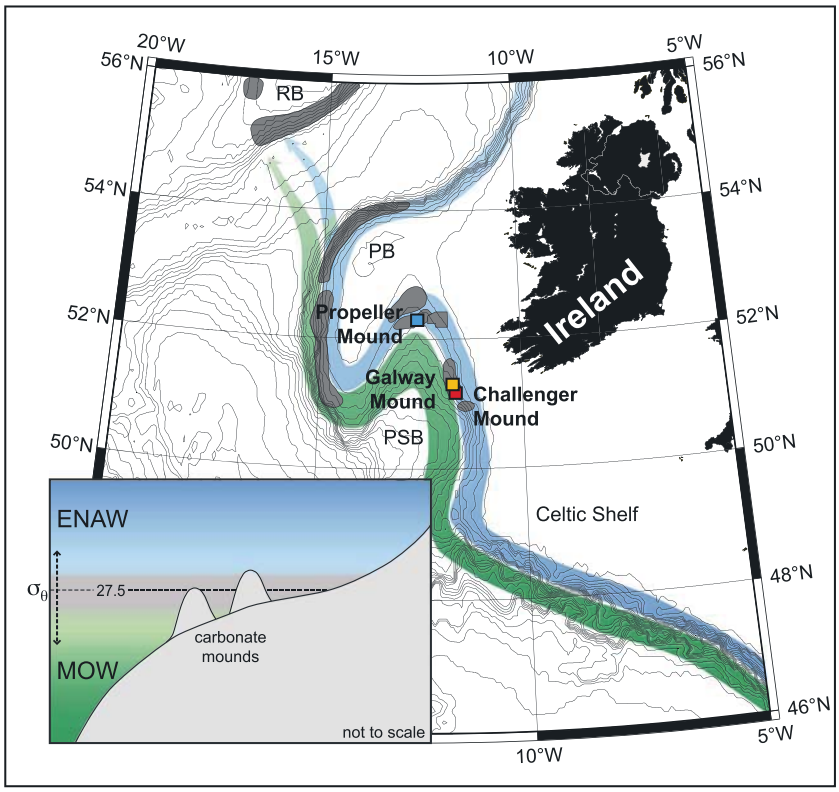

Figure 1. Locations of investigated carbonate mounds, intermediate water mass circulation, and carbonate mound provinces (grey areas) within the Porcupine Seabight. Depth lines correspond to 200 m intervals, PB = Porcupine Bank, PSB = Porcupine Seabight, RB = Rockall Bank. Sketch illustrates present water mass configuration along the slopes of the Porcupine Seabight or Bank (not to scale). Eastern North Atlantic Water (ENAW, blue) overlies Mediterranean Outflow Water (MOW, green). The position of the pycnocline ($\sigma_\Theta = 27.5$) varied during the past ~3 Myr being shallower during peak glacial (e.g., Last Glacial Maximum) or deeper during peak interglacial periods (e.g., Holocene and Marine Isotope Stage 5.5) or in times before the Northern Hemisphere glaciation (>2.7 Ma).

distribution [e.g., *Maier et al*., 2011; *Form and Riebesell*, 2012; *Thiagarajan et al*., 2013; *Flögel et al*., 2014]. However, as corals also depend on particulate organic matter and zooplankton as prime nutrition, it was argued that their distribution along the European continental margin follows distinct water mass signatures and their dynamical regimes [*Freiwald*, 2002; *De Mol et al*., 2002, 2005; *White*, 2007]. Detailed regional and local oceanographic studies have shown the significance of physical parameters on living CWC reef occurrences [*Davies et al*., 2008; *White and Dorschel*, 2010] among which the potential seawater density (σ_Θ) referenced to the surface appears to be a key factor [*Dullo et al*., 2008]. At present, all prolific growing CWC reefs (Category I in the sense of *Flögel et al*. [2014]) along the European continental margin from the Iberian margin (42°N), the Porcupine Seabight (50°N), to northern Norway (70°N) are found in a density range of $\sigma_\Theta = 27.35$–$27.65\ \mathrm{kg\ m^{-3}}$ [*De Mol et al*., 2011; *Flögel et al*., 2014; *Somoza et al*., 2014; *Sánchez et al*., 2014]. This density range is also characterized by a steep gradient, which is an increase in seawater density within a short bathymetric range [*Dullo et al*., 2008; *Hebbeln et al*., 2014], favoring the widespread development of nepheloid layers [*Dickson and McCave*, 1986; *Rice et al*., 1991; *Mazzini et al*., 2012]. Due to this pycnocline, horizontal currents develop and internal waves may propagate carrying nutrition and may even influence the distribution of larvae [*Dullo et al*., 2008; *Henry et al*., 2014]. Past variations of seawater density, especially across glacial-interglacial cycles, have been documented by, e.g., *Dokken and Jansen* [1999], *Lynch-Stieglitz et al*. [1999a, 1999b], or *Peck et al*. [2006] indicating a dynamic and variable environment at depths.

The aim of this study is (1) to test regionally calibrated equations to reconstruct seawater densities following the method of *Lynch-Stieglitz et al*. [1999a, 1999b] and based on this (2) to test whether CWC mound growth during the past also occurred in similar seawater densities as today. To answer these questions, we analyzed sediment

cores and reconstructed seawater densities from two different and well-studied carbonate mounds; Propeller Mound of the Hovland mound province, northern Porcupine Seabight [e.g., *Dorschel et al*., 2005, 2007; *Rüggeberg et al*., 2005, 2007; *Beuck and Freiwald*, 2005; *Heindel et al*., 2010; *Schönfeld et al*., 2011], and Challenger Mound of the Belgica mound province, eastern Porcupine Seabight [e.g., *Foubert et al*., 2005; *Williams et al*., 2006; *Kano et al*., 2007; *Thierens et al*., 2010; *Titschack et al*., 2009] (Figure 1).

2. Approach

2.1. Age Determination and Stratigraphic Framework

2.1.1. Sample Preparation

In several depth intervals of core GeoB 6730-1 coral fragments of *Lophelia pertusa* were selected to determine absolute age data using the U/Th isotope systematic of the aragonite skeleton. The selection followed first interpretations of sedimentological data and stable isotopes on foraminifera [*Dorschel et al*., 2005; *Rüggeberg et al*., 2007] and before or after identified hiatuses [*Dorschel et al*., 2005]. All coral samples were first rigorously mechanically cleaned with dental-technical driller and abrasion tools down to millimeter-sized fragments of massive aragonitic internal skeleton parts and repeatedly ultrasonified in MQ-water ($>$18 MΩ) in order to remove remnants of exterior contaminants (sediments, iron-manganese crusts, and coatings). Each precleaned fragment was bathed in 50/50 mixture of 30% H_2O_2 and 1 *M* NaOH and MQ-water alternately for 15 min with ultrasonification [*Cheng et al*., 2000a]. This procedure was performed up to three times to ensure high removal rates for particles, organic stains, and oxides potentially left after mechanical procedure on the coral and within the open pore space surfaces. However, the last $HClO_4$ cleaning step described by *Cheng et al*. [2000a] was skipped due to the related risk of increased sample loss on small fragments. Before element separation, all samples were checked again for the cleanness and purely aragonitic crystal structures under the binocular. Element separation procedure was based on Eichrom-UTEVA resin (according to manufacturer notes and *Fietzke et al*. [2005]).

X-ray diffraction (XRD) on selected samples additionally helped to determine calcite content to be below the detection limit ($<$2%, defined by an artificial calibration mixture). All subsamples for XRD measurements were taken with a microdriller from freshly cut surfaces of cleaned fragments of *L. pertusa*, after discarding first drill steps as additional surface cleaning procedure.

2.1.2. Uranium-Series Geochronology

Uranium-series measurements for U/Th coral ages were performed at GEOMAR Helmholtz Centre for Ocean Research Kiel, Germany, on a Finnigan MAT 262 RPQ+ (Mat262), a Thermo-Finnigan Triton-RPQ (Triton) thermal ionization mass spectrometer (TIMS), and a VG Axiom multicollector inductively coupled plasma mass spectrometer (MC-ICP-MS) applying lab procedures and methods of *Fietzke et al*. [2005] and *Edwards et al*. [1986], and decay constants of *Cheng et al*. [2000b]. Sample 6730/108 (Table S1 in the supporting information) is measured twice for Th with MC-ICP-MS in independent sessions (Axiom 1 and 2) and for U with TIMS (MAT262 and Triton) and MC-ICP-MS as well. The resulting mean value of multiple measurements reflects reproducibility and robustness of applied methods.

For isotope dilution measurements a combined $^{233/236}U/^{229}Th$ spike was used, with stock solutions calibrated for concentration using NIST-SRM 3164 (U) and National Institute of Standards and Technology-Standard Reference Material (NIST-SRM) 3159 (Th), as combi-spike calibrated against CRM-145 uranium standard solution (also known as NBL-112A) for U isotope composition and against a secular equilibrium standard (HU-1, uranium ore solution) for determination of $^{230}Th/^{234}U$ activity ratio. Characteristic whole procedure blanks at time of sample preparation were around 14 to 60 pg for U, 6 to 9 pg for ^{232}Th, and 0.5 to 5 fg for ^{230}Th. Calculation of geochronological data and activity ratios is based on the decay constants published by *Cheng et al*. [2000b] (further details, see supporting information).

The applied data reduction includes a correction for isotopic composition of incorporated Th of detrital origin, according to continental crust values [*Wedepohl*, 1995] as approximation for potentially involved shelf sediments (details given in Table S1 in the supporting information). In most cases this correction is negligible due to sufficiently high $^{230}Th/^{232}Th$ activity ratios and low Th concentrations in the corals. Due to the generally high ages in this sample set, the impact of age correction on the interpretation of $\delta^{234}U$ values is significant and criteria for isotopic reliability of ^{230}Th age data may be applied. Recent reef forming cold-water corals showed within their uncertainties similar $\delta^{234}U_{(0)}$ values of 145.5 ± 2.3‰ [*Cheng et al*., 2000a] and

146.3 ± 3.9‰ [*Liebetrau et al*., 2010] for different depth and location, supporting the application of the $\delta^{234}U_{(T)}$ reliability criteria presented for cold-water corals by different studies (e.g., 145.5–148.3‰: *Robinson et al*. [2004]; 146.2 ± 3.4‰: *Frank et al*. [2004]; 146 ± 7‰: *López Correa et al*. [2012], *McCulloch et al*. [2010], and *Robinson et al*. [2007]; 146 ± 15‰: *Eisele et al*. [2011]). *Wienberg et al*. [2010] used the criteria in the style of *Blanchon et al*. [2009] but for CWC with strictly reliable (SR) for $\delta^{234}U_{(T)}$ = 146.6–149.6‰, reliable (R) for $\delta^{234}U_{(T)}$ = 149 ± 10‰, and not reliable (NR) for $\delta^{234}U_{(T)}$ values below 139‰ and above 159‰. We also follow these criteria in this study (Figure S1 and Table S1).

Regarding the application of $\delta^{234}U_{(T)}$ reliability criteria on U-Th data sets of CWCs covering interglacial and glacial time intervals, a constant and homogeneous $\delta^{234}U$ value throughout the water column and across major changes in continental runoff is a prerequisite. Noteworthy, only a few data points from glacial periods have been reported suggesting initial $\delta^{234}U_{(T)}$ was as low as 136‰ during most of the past glaciation [*Thompson et al*., 2003]. However, the majority of our $\delta^{234}U_{(T)}$ data set is in general accordance with the published reliability criteria. Due to sorrowful selection of massive and pristine appearing coral fragments combined with rigorous cleaning procedures, 9 of 11 analyzed samples reached the reliable ("R") or even strictly reliable ("SR") level (Table S1) and could be considered for geochronological interpretation (Figure 4). The two samples with clearly deviating values of 119 and 164‰ (Table S1 and Figure S1), respectively, provide data set integrity and are regarded as examples for the diagenetic impact of carbonate-rich fluids potentially percolating within the porous mound structures around buried reef fragments. Four samples (6730-1: 18 cm, 68 cm, 178 cm, and 318 cm) are characterized by elevated Th concentrations (>50 ppb) and consequently accompanied by slightly enlarged age uncertainty and reduced age reliability. Conservatively, these dates should be considered as maximum ages.

Due to two observations and its general importance, the highest age of the record determined for 318 cm core depth (sample 6730-1/318, 296 ± 18 kyr B.P.) is given in italics (1) but still considered (2) in Figure 4 and discussed in detail below:

1. Its $\delta^{234}U_{(T)}$ value of 139.4 ± 9.9‰ is slightly to low and reaches the highest quality level SR only by taking the unusual large uncertainty into account. The latter is mainly introduced by the high Th content (>100 ppb) and the subsequently high impact of the error propagation from the uncertainty of detrital correction (supporting information Text S1) on the U-Th age (T), providing the basis for the $\delta^{234}U_{(T)}$ calculation.
2. The calculation of the completely Th independent ^{234}U excess age, considering an initial $\delta^{234}U_{(T)}$ value of 146 ± 2‰ of modern seawater [*Henderson and Anderson*, 2003] as reasonable starting point, ends up in an age of 314 ± 15 kyr B.P., overlapping with the U-Th age at similar precision. This age corresponds to the time span required for the decay of the unsupported (excess) ^{234}U of the initially incorporated U down to the today measured $^{234}U/^{238}U$ activity ratio and is determined by ($T = (1/\lambda^{234}U) \times LN\ (\delta^{234}U_{(modern\ seawater)}/\delta^{234}U_{(sample\ measured)})$).

In addition to this less precise but robust accordance of two chronometer, the slightly low $\delta^{234}U_{(T)}$ of the U-Th age could be interpreted following suggestions in *Thompson et al*. [2003] concerning glacial periods which may provide lower $\delta^{234}U$ values when compared to interglacial and modern ocean signatures. Consequently, the $\delta^{234}U_{(T)}$ reliability criteria applied by *Wienberg et al*. [2010] for CWC and *Blanchon et al*. [2009] for tropical corals would be not perfectly adequate or even misleading for samples of marine glacial carbonates. However, the remarkable age around 300 kyr is pointing to cold-water coral growth at the transition from the late MIS 9 (9.1) interglacial to the early MIS 8 (8.4) glacial period. Due to the slight difference between the mean U-Th and $^{234}U_{(exc.)}$ ages and their range of uncertainty, a clear discrimination between both stages cannot be given based on the actual data set.

Independently and by far more precise, the U-Th age of 176 ± 3 kyr B.P. at 178 cm core depth is reflecting CWC growth at early MIS 6.5 according the LR04 stack [*Lisiecki and Raymo*, 2005]. However, the 178 cm data do not reflect any indication of lower $\delta^{234}U$ values (149.8 ± 3.4‰ $\delta^{234}U_{(T)}$) as suggested for glacial periods [*Thompson et al*., 2003].

2.1.3. Stratigraphic Framework

Absolute ages of CWC *L. pertusa* and additional U/Th dates of corals and AMS^{14}C dates from sediments of Propeller Mound, Galway Mound, and Challenger Mound were collected from published studies [*Dorschel et al*., 2005; *Eisele et al*., 2008; *Frank et al*., 2011; *Raddatz et al*., 2014] (Table 1) and used to identify phases of carbonate mound growth and decline in comparison to the LR04 marine isotope stack of *Lisiecki and*

Table 1. Age Data, Corresponding $\delta^{18}O_C$ Values, and Calculated Seawater Densities[a]

Sample	Depth (cm)	Age (kyr B.P.)	Error (kyr)	Reference	Method	$\delta^{18}O_C$ (‰ VPDB)	Reference	Seawater Density (kg/m^3) Interglacial Equation (3)	Intermediate Equation (7)	Glacial Equation (6)
HMP	BW	0	–	This study	–	1.48[b]	This study	**27.4**	27.2	26.6
BMP	BW	0	–	This study	–	1.68[b]	This study	**27.5**	27.3	26.8
IODP1317C	10	1.2	0.1	Raddatz *et al.* [2014]	Coral U-Th	1.33	Raddatz *et al.* [2011]	**27.2**	27.1	26.4
GeoB6730-1	3	1.9	0.1	This study	Coral U-Th	1.49	Dorschel *et al.* [2005]	**27.4**	27.2	26.6
GeoB6730-1	23	4.5	0.1	Dorschel *et al.* [2005]	Sed-14C	1.5	Dorschel *et al.* [2005]	**27.4**	27.2	26.6
GeoB6730-1	18	5.2	0.1	This study	Coral U-Th	1.45	Dorschel *et al.* [2005]	**27.3**	27.1	26.5
GeoB9223-1	168	5.5	0.1	Frank *et al.* [2011]	Coral U-Th	1.55	Eisele *et al.* [2008]	**27.4**	27.2	26.6
GeoB9214-1	178	7.3	0.1	Eisele *et al.* [2008]	Sed-14C	1.56	Eisele *et al.* [2008]	**27.4**	27.2	26.7
GeoB9213-1	143	8.3	0.1	Eisele *et al.* [2008]	Sed-14C	1.57	Eisele *et al.* [2008]	**27.4**	27.2	26.7
GeoB9214-1	213	8.7	0.1	Eisele *et al.* [2008]	Sed-14C	1.44	Eisele *et al.* [2008]	**27.3**	27.1	26.5
GeoB9214-1	180	8.7	0.2	Frank *et al.* [2004]	Coral U-Th	1.66[c]	Eisele *et al.* [2008]	**27.5**	27.3	26.8
GeoB9213-1	150	9.2	0.2	Frank *et al.* [2004]	Coral U-Th	1.58[d]	Eisele *et al.* [2008]	**27.4**	27.2	26.7
GeoB6719-1	98	18.6	0.6	Dorschel *et al.* [2005]	Sed-14C	3.54	Dorschel *et al.* [2005]	28.3	27.7	**28.0**
GeoB6725-1	168	23.5	0.8	Dorschel *et al.* [2005]	Sed-14C	3.61	Dorschel *et al.* [2005]	28.3	27.7	**28.0**
GeoB6719-1	163	25.4	1	Dorschel *et al.* [2005]	Sed-14C	3.45	Dorschel *et al.* [2005]	28.3	27.7	**28.0**
GeoB6719-1	273	30.8	0.7	Dorschel *et al.* [2005]	Sed-14C	3.13	Dorschel *et al.* [2005]	28.2	27.7	**27.8**
GeoB6729-1	23	55	1	Dorschel *et al.* [2005] and this study	Coral U-Th	2.85	Dorschel *et al.* [2005]	28.1	**27.6**	27.7
GeoB6730-1	68	97	2	This study	Coral U-Th	2.21	Dorschel *et al.* [2005]	27.8	**27.5**	27.2
GeoB6730-1	58	99	1	This study	Coral U-Th	1.84	Dorschel *et al.* [2005]	27.6	**27.3**	26.9
IODP1317C	475	105	1	Raddatz *et al.* [2014]	Coral U-Th	n.d.	–	–	–	–
GeoB6730-1	108	111	2	This study	Coral U-Th	2.27	Dorschel *et al.* [2005]	27.9	**27.5**	27.3
GeoB6730-1	108	112	1	This study	Coral U-Th	2.27	Dorschel *et al.* [2005]	27.9	**27.5**	27.3
GeoB6730-1	108	112	1	This study	Coral U-Th	2.27	Dorschel *et al.* [2005]	27.9	**27.5**	27.3
GeoB6730-1	108	112	1	This study	Coral U-Th	2.27	Dorschel *et al.* [2005]	27.9	**27.5**	27.3
GeoB9214-1	281	129	1	Frank *et al.* [2011]	Coral U-Th	1.68	Eisele *et al.* [2008]	**27.5**	27.3	26.8
GeoB6728-1	3	152	3	Dorschel *et al.* [2005] and this study	Coral U-Th	3.27	Dorschel *et al.* [2005]	28.3	**27.7**	27.9
GeoB6730-1	178	176	3	This study	Coral U-Th	2.43	Dorschel *et al.* [2005]	28.0	**27.6**	27.4
GeoB6729-1	73	184	4	Dorschel *et al.* [2005] and this study	Coral U-Th	3.06	Dorschel *et al.* [2005]	28.2	**27.7**	27.8
GeoB6728-1	83	193	4	Dorschel *et al.* [2005] and this study	Coral U-Th	3.28	Dorschel *et al.* [2005]	28.3	**27.7**	27.9
GeoB6730-1	238	204	5	This study	Coral U-Th	2.25	Dorschel *et al.* [2005]	27.7	**27.5**	27.3
GeoB6728-1	218	229	6	Dorschel *et al.* [2005] and this study	Coral U-Th	2.47	Dorschel *et al.* [2005]	28.0	**27.6**	27.4
GeoB6730-1	273	240	6	This study	Coral U-Th	1.78[e]	Dorschel *et al.* [2005]	**27.6**	27.3	26.9
GeoB9214-1	378	269	9	Frank *et al.* [2004]	Coral U-Th	1.39	Eisele *et al.* [2008]	**27.3**	27.1	26.5
GeoB9213-1	385	277	5	Eisele *et al.* [2008]	Coral U-Th	2.28[f]	Eisele *et al.* [2008]	27.9	**27.5**	27.3
GeoB6730-1	318	296	18	This study	Coral U-Th	2.89	Dorschel *et al.* [2005]	28.2	**27.6**	27.7
GeoB6728-1	368	300	11	Dorschel *et al.* [2005] and this study	Coral U-Th	1.72	Dorschel *et al.* [2005]	**27.5**	27.3	26.8
GeoB9213-1	462	300	12	Eisele *et al.* [2008]	Coral U-Th	1.69[g]	Eisele *et al.* [2008]	**27.5**	27.3	26.8
IODP1317C	2,018	386	25	Raddatz *et al.* [2014]	Coral U-U	1.91	Raddatz *et al.* [2011]	27.7	**27.4**	27.0
IODP1317C	2,274	426	37	Raddatz *et al.* [2014]	Coral U-U	2.33	Raddatz *et al.* [2011]	27.9	**27.5**	27.3
IODP1317C	2,869	1,670	+220/-150	Raddatz *et al.* [2014]	Coral $^{87/88}Sr$	2.44	Raddatz *et al.* [2011]	28.0	**27.6**	27.4

Table 1. (continued)

Sample	Depth (cm)	Age (kyr B.P.)	Error (kyr)	Reference	Method	$\delta^{18}O_C$ (‰ VPDB)	Reference	Seawater Density (kg/m^3) Interglacial Equation (3)	Intermediate Equation (7)	Glacial Equation (6)
IODP1317C	14,569	2,930	+1260/-530	Raddatz *et al.* [2014]	Coral $^{87/88}Sr$	1.95[h]	Raddatz *et al.* [2011]	27.7	**27.4**	27.0

[a]Data compilation of coral ages (Coral U-Th, U-U, $^{87/88}Sr$) on Lophelia pertusa and sediment ages (Sed-14C) with corresponding $\delta^{18}O_C$ values of benthic foraminifera (see Figure 2) and calculated potential seawater densities using equations for peak interglacial (equation (3)), peak glacial (equation (6)), and intermediate (equation (7)) settings. Bold numbers correspond to accepted values for the time period and equation used. HMP = Hovland Mound Province, BMP = Belgica Mound Province, BW = bottom water.
[b]Reconstructed $\delta^{18}O_C$ using relation of Marchitto *et al.* [2014] (equation (2)) and own $\delta^{18}O_{SW}$, salinity, and temperature data.
[c]$\delta^{18}O_C$ value from 183 cm core depth.
[d]$\delta^{18}O_C$ value from 148 cm core depth.
[e]$\delta^{18}O_C$ value from 268 cm core depth.
[f]$\delta^{18}O_C$ value from 388 cm core depth.
[g]$\delta^{18}O_C$ value from 463 cm core depth.
[h]$\delta^{18}O_C$ value from 14565 cm core depth.

Raymo [2005] (Figure 2). Stable oxygen isotope values for the absolutely dated corals derive from calcite tests of epibenthic foraminifera ($\delta^{18}O_C$) from the same depth interval of the coral within the core (Table 1 and Figure 2). We use the generalized glacial-interglacial cycles as consisting of three quite distinct settings (*peak interglacial*, *peak glacial*, and *intermediate settings*, Figure 2), similar to other studies [e.g., *Peacock et al.*, 2006]. Peak glacial corresponds to the Last Glacial Maximum (LGM) and similar periods of low sea level stand, cold conditions, and high sediment input with typical benthic $\delta^{18}O_C$ values of $> 3.2‰$ for the study area. Peak interglacial periods are those such as the Holocene, where sea level was high, warm conditions prevailed and benthic $\delta^{18}O_C$ values of $< 1.9‰$ are common. The *intermediate* stage corresponds to the periods between peak glacial and peak interglacial phases, roughly the moderate glacial and interglacial phases as well as the interstadials (warm glacial periods), where benthic $\delta^{18}O_C$ values lay between 1.9 and 3.2‰ (Figure 2).

2.1.4. Error Analysis

One source of errors is the uncertainty between sediment and coral age. Especially at hiatuses strong mixing of sediment averages time, which can attain several millennia [*López Correa et al.*, 2012]. Age differences reported from carbonate mounds of the Rockall Bank and Porcupine Seabight are generally ~500–1000 years, occasionally up to 2000 years [*Lutringer et al.*, 2005; *Eisele et al.*, 2008; *Mienis et al.*, 2009; *de Haas et al.*, 2009]. These differences are within the age uncertainty of investigated samples older than 50 ka (Table 1). Only one larger age difference of ~40 kyr (AMS ^{14}C age of 45 ka compared to U-Th date of 93 ka) has been published so far from sediments covering a big hiatus [*Dorschel et al.*, 2005]. This has been interpreted by enhanced coral growth supported by strong currents followed by a period with weaker currents allowing the deposition of fine sediments among the older coral framework. Therefore, for data close to a hiatus possible large age offsets should be taken into consideration. The presented data set in Figure 2 exhibits only one sample at 269 ka, which does not fit to the oxygen isotope record (offset ~1.5‰) implying a hiatus as a result of reworking. All other samples, however, fit to the curve of LR04, even in older parts within the error bars (Figure 2).

2.2. Determination of Past Seawater Density

In order to determine past seawater densities, we followed the established approach of *Lynch-Stieglitz et al.* [1999a, 1999b], using stable oxygen isotopes of calcite tests ($\delta^{18}O_C$) of epibenthic foraminifera from carbonate mound sediments. This reconstruction is based on the fact that a change of seawater density and $\delta^{18}O_C$ is driven by two independent parameters: salinity (evaporation and precipitation) and temperature (ice volume). The dependency of seawater density on salinity and temperature is

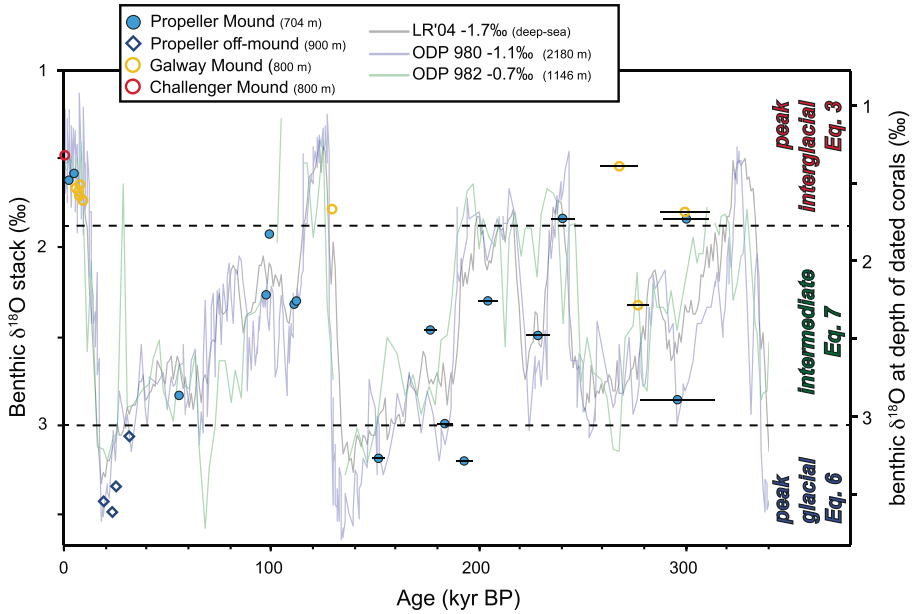

Figure 2. Comparison of $\delta^{18}O_C$ of benthic foraminifera at depths of U-Th dated coral fragments (*L. pertusa*) and AMS^{14}C dated sediments (Last Glacial Maximum) from different carbonate mounds (700–800 m water depths) of the past 300 kyr with benthic $\delta^{18}O$ records of *Lisiecki and Raymo* [2005] (black curve), ODP Leg 980 from 2180 m water depth [*Oppo et al.*, 2006] (blue curve), and ODP Leg 982 from 1146 m water depths [*Venz et al.*, 1999] (green curve). Please note that these records are adjusted by −1.7, −1.1, and −0.7 ‰, respectively, to align with the core data from the Porcupine Seabight. Age uncertainty is smaller than the symbol for ages < 130 ka or indicated by horizontal bars (>MIS 6), precision of $\delta^{18}O_C$ data is 0.07‰. Horizontal dotted lines indicate the division into peak glacial, intermediate, and peak interglacial settings with their respective equations (further details, see text).

assumed to be constant throughout the oceans and geological time [*Lynch-Stieglitz et al.*, 1999a]. Eight different equations were proposed to reconstruct paleoseawater densities from $\delta^{18}O_C$ accounting for different oceanographic settings and temperature regimes [*Lynch-Stieglitz et al.*, 1999b]. Based on these equations, we developed regionally fitted equations for the Porcupine Seabight using bottom water temperature, salinity, seawater density, and stable oxygen isotope data of seawater ($\delta^{18}O_{SW}$) from research cruises with R/V *METEOR* M61/1 and M61/3, R/V *POSEIDON* P316, and data from the Global Seawater Oxygen 18 Database [*Schmidt et al.*, 1999]. Recent $\delta^{18}O_{SW}$ to salinity (S) relationship (Figure S2 and Table S2) for the Porcupine Seabight is expressed in equation (1) (Figure 3a):

$$\delta^{18}O_{SW} = 0.446 \times S - 15.39 \qquad R^2 = 0.44 \tag{1}$$

Following *Lynch-Stieglitz et al.* [1999b] we calculated $\delta^{18}O_C$ using the recently developed $\delta^{18}O_C/\delta^{18}O_{SW}$-temperature relation of *Marchitto et al.* [2014]. This equation is based on the calibration of *Cibicides* and *Planulina* $\delta^{18}O_C$ data from Atlantic, Pacific, and Arctic sites covering a temperature range of −1 to +26°C given in equation (2) for recent values:

$$\delta^{18}O_C = \left(\delta^{18}O_{SW} - 0.27\right) - 0.224 \times T + 3.53 \qquad R^2 = 0.99 \tag{2}$$

The present-day, regional (PSB) $\delta^{18}O_{SW}$ and temperature data (Table S2) were used to determine $\delta^{18}O_C$ values, which are in good agreement with recent epibenthic $\delta^{18}O_C$ values. Therefore, we also used this equation to estimate temperature ranges for the investigated time intervals (see supporting information Text S3 and Tables S4 and S5). The recent calculated $\delta^{18}O_C$ and measured σ_Θ values give the relation expressed in equation (3), which we applied for the reconstruction of seawater densities for the Holocene and equivalent peak interglacial periods (see Figure 3b):

$$\sigma_\Theta = 25.86 + 1.23 \times \delta^{18}O_C - 0.15 \times \delta^{18}O_C{}^2 \qquad R^2 = 0.91 \tag{3}$$

Difference between calculated and measured seawater densities for the recent calibration is relatively small with ±0.06 kg m^{-3} (Table S2).

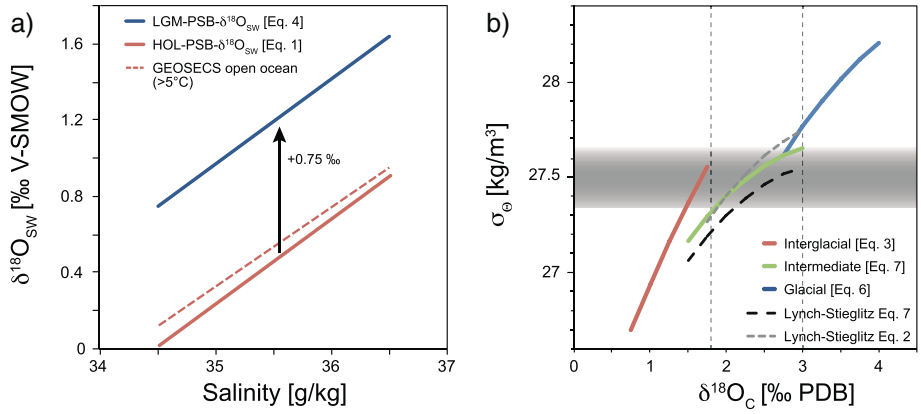

Figure 3. (a) $\delta^{18}O_{SW}$-salinity relation for the recent Porcupine Seabight in comparison with GEOSECS stations (from Global Seawater Oxygen-18 Database) [*Schmidt et al.*, 1999] and the regional Last Glacial Maximum (LGM) $\delta^{18}O_{SW}$-salinity relation (see text for detailed explanation). (b) Regional $\delta^{18}O_C$-potential seawater density relation for *peak interglacials* (based on the recent calibration, <1.8‰), peak glacials (based on LGM calibration, >3‰), and intermediate for the times between peak glacials and *interglacials* (see Figure 2) in comparison to relations determined by *Lynch-Stieglitz et al.* [1999b] of Global Open Ocean calibration (equation (2)) or its modifications with 4‰ higher fresh end-member (equation (7)).

For *peak glacials* such as the Last Glacial Maximum (LGM) we derived temperatures (T_{LGM}) and salinities (S_{LGM}) from model data (PMIP2 HadCM3M2, *Braconnot et al.* [2007], and Table S3) and calculated seawater densities ($\sigma_{\Theta\text{-LGM}}$). We used S_{LGM} data and applied equation (1) to determine $\delta^{18}O_{SW\text{-LGM}}$, which was corrected by 0.75‰ following the considerations of *Schrag et al.* [2002] (Figure 3a):

$$\delta^{18}O_{SW\text{-LGM}} = 0.446 \times S_{LGM} - [15.39 + 0.75] \tag{4}$$

Consequently, $\delta^{18}O_{C\text{-LGM}}$ was determined using equation (2) but for LGM values:

$$\delta^{18}O_{C\text{-LGM}} = \left(\delta^{18}O_{SW\text{-LGM}} - 0.27\right) - 0.224 \times T_{LGM} + 3.53 \tag{5}$$

Analogously to equation (3) we derived seawater densities from $\delta^{18}O_{C\text{-LGM}}$ to determine the relation between $\delta^{18}O_{C\text{-LGM}}$ and $\sigma_{\Theta\text{-LGM}}$ given in equation (6) (Figure 3b):

$$\sigma_{\Theta\text{-LGM}} = 24.80 + 1.41 \times \delta^{18}O_C - 0.14 \times \delta^{18}O_C{}^2 \tag{6}$$

Modeled LGM seawater densities at 667 m of 27.7 kg m^{-3} (Table S3) are slightly lighter but also shallower and from different age compared to the reconstructed values based on $\delta^{18}O_{C\text{-LGM}}$ of 28.0 at 760 m (18.6 kyr B.P.) and 28.1 kg m^{-3} at 820 m (23.5 kyr B.P.), respectively (Table 1).

For the intermediate time intervals we developed a best estimate equation (equation (7)). This equation is a reasonable estimation comparable to the Global Open Ocean calibration or its modifications with 4‰ higher fresh end-member of *Lynch-Stieglitz et al.* [1999b]. Since there are no local and regional transient model data covering the interval available for temperature and salinity nor equivalent proxy-based calculations for the depth interval of interest, this best nonlinear estimate links the defined warm and cold end-member estimates (Figure 3b):

$$\sigma_{\Theta\text{-Intermediate}} = 26.0 + 1.0 \times \delta^{18}O_C - 0.15 \times \delta^{18}O_C{}^2 \tag{7}$$

The onset of mound growth ~2.7 Ma coincides with the beginning of the Northern Hemisphere glaciation [*Haug and Tiedemann*, 1998]. This early phase of mound growth, however, was characterized by oceanographic and climatic conditions close to those of interglacials [*Thierens et al.*, 2010; *Raddatz et al.*, 2011], with most of the $\delta^{18}O_C$ values correlating with the upper range of our intermediate setting [*Lisiecki and Raymo*, 2005, 2007]. Therefore, we use equation (7) for paleoseawater reconstruction of carbonate mound development back to the early initiation at around 2.7 Ma. We applied the same equation to the Miocene sediments below the mound base for comparative reason. However, the method for reconstructing seawater densities as described by *Lynch-Stieglitz et al.* [1999b] might not be applicable for middle Miocene sediments and should be therefore treated with caution.

The relation between seawater density and CWC growth is interpreted only on larger time scales, especially taking the large age error at mound initiation based on Sr-isotope stratigraphy into account, which does not allow the discussion on small time scales and in high resolution, yet. Investigated sediment core of Propeller Mound covers the past ~300 kyr while samples of IODP 307 Site U1317C on Challenger Mound have a middle Miocene age below the mound base and a late Pliocene/early Pleistocene age of ~2.7 Ma above the mound base [*Kano et al*., 2007; *Raddatz et al*., 2014]. The error for paleoseawater densities is relatively low due to the combined effect of temperature and salinity on $\delta^{18}O_C$. At higher temperatures, lines of constant $\delta^{18}O_c$ and lines of constant potential density anomaly are roughly parallel [*Lynch-Stieglitz et al*., 1999b], but deviation between the lines increases with decreasing temperature, especially below 5°C. Therefore, we established a regional glacial equation (equation (6)) based on modeled data (PMIP2 HadCM3, [*Braconnot et al*., 2007]), which is in reasonable agreement with measured $\delta^{18}O_c$ of benthic foraminifera from the last glacial period, but also underlining the difficulties of reconstructions at low temperatures. The error estimate of the recent calibration is relatively small with $\Delta\sigma_\Theta = 0.06\,\mathrm{kg\,m^{-3}}$, but we expect a slightly larger error of $\Delta\sigma_\Theta = 0.1$–$0.15\,\mathrm{kg\,m^{-3}}$ for the paleoreconstruction.

3. Results and Discussion

3.1. Cold-Water Coral Reef Development During the Past 300,000 Years

The studied core from the top of Propeller Mound is 350 cm long. According to the U-Th geochronology of 11 CWC fragments (*Lophelia pertusa*), the core dates back to approximately MIS 9.1 (MIS 8.4–9.2, ~300 ka; Figure 4a). Several well-recognized hiatuses, indicated by dashed lines in Figure 4a, comprise times of non-deposition equivalent to time intervals of no CWC reef growth and subordinate erosion [*Dorschel et al*., 2005]. The uppermost part represents the Holocene (MIS 1) with mean σ_θ values of $27.3\,\mathrm{kg\,m^{-3}}$, indicating a rather marginal position on the envelope defined for prolific recent CWC reef growth of category I in the sense of *Flögel et al*. [2014], which is characterized by a horizontal area covered with living CWCs of several $100\,\mathrm{m^2}$ and a distinct vertical elevation due to biogenic frame building. In the Hovland mound province Propeller Mound is situated in a slightly shallower bathymetric range (690–710 m water depths) [*Rüggeberg et al*., 2007] with the present-day seawater density values of $27.4\,\mathrm{kg\,m^{-3}}$ (Table S2) compared to the active coral growth in the Belgica mound province at, e.g., Galway Mound (780–950 m water depths, *Dorschel et al*. [2007]; present-day σ_θ values of $27.5\,\mathrm{kg\,m^{-3}}$, Table S2). The first hiatus in Propeller Mound covers the time interval between MIS 2 and MIS 5.2 (Figure 4a). The section below, MIS 5.3 and 5.4, documents active CWC reef growth under reconstructed σ_θ values of $27.4\,\mathrm{kg\,m^{-3}}$. Based on our age data and the LR04 marine isotope stack [*Lisiecki and Raymo*, 2005], the second hiatus covers the time from MIS 5.5 to MIS 6.4. Although MIS 6 represents a glacial period, there is one warmer phase defined as MIS 6.5 (Figure 2). Propeller Mound recorded that specific time window by active accumulation reflecting characteristic σ_θ values of $27.5\,\mathrm{kg\,m^{-3}}$ and cold-water coral growth with an age of 176 ± 3 ka at 178 cm core depth for the basal layer above another hiatus (Figure 4a). The interglacial stage of MIS 7 displays prolific CWC reef growth of more than 1 m having mean σ_θ values of $27.4\,\mathrm{kg\,m^{-3}}$ back to an age of 204 ± 5 ka. Prior to this time, there is still CWC reef growth but more on a marginal position of the σ_θ envelope illustrated by minor coral contributions to silty sediments [*Rüggeberg et al*., 2007]. The lowermost section of the core has a calculated σ_θ range of 27.3–$27.6\,\mathrm{kg\,m^{-3}}$. The upper part, from 273 down to 318 cm, is interrupted by a hiatus around 303 cm. Below the reconstructed σ_θ values have a mean of $27.6\,\mathrm{kg\,m^{-3}}$. The U-Th systematic implies an age of cold-water coral formation around 300 ka covering (within uncertainty) the glacial/interglacial transition between MIS 9.1 and MIS 8.5 (Table S1). The corresponding core section is generally characterized by minor coral content [*Rüggeberg et al*., 2007] with intercalated layers enriched in small coral fragments (Figure 4a).

Based on U-Th-series ages of cold-water corals of the NE Atlantic region, *Frank et al*. [2011] suggested a strong climatic influence on the geographical distribution and the sustained development over the past three glacial-interglacial cycles. They showed that middepth temperatures and primary productivity might play a crucial role as drivers of these ecosystems. *Rüggeberg et al*. [2007] already presented the existence of a well-expressed pycnocline (density gradient) as important parameter for the CWC ecosystem. This was subsequently identified as an important factor in understanding the recent distribution of cold-water coral reefs in the NE Atlantic [*Dullo et al*., 2008; *De Mol et al*., 2011; *Rüggeberg et al*., 2011; *Flögel et al*., 2014] and the Gulf of Mexico [*Hübscher et al*., 2010; *Hebbeln et al*., 2014]. Here we argue that the pycnocline represented by the

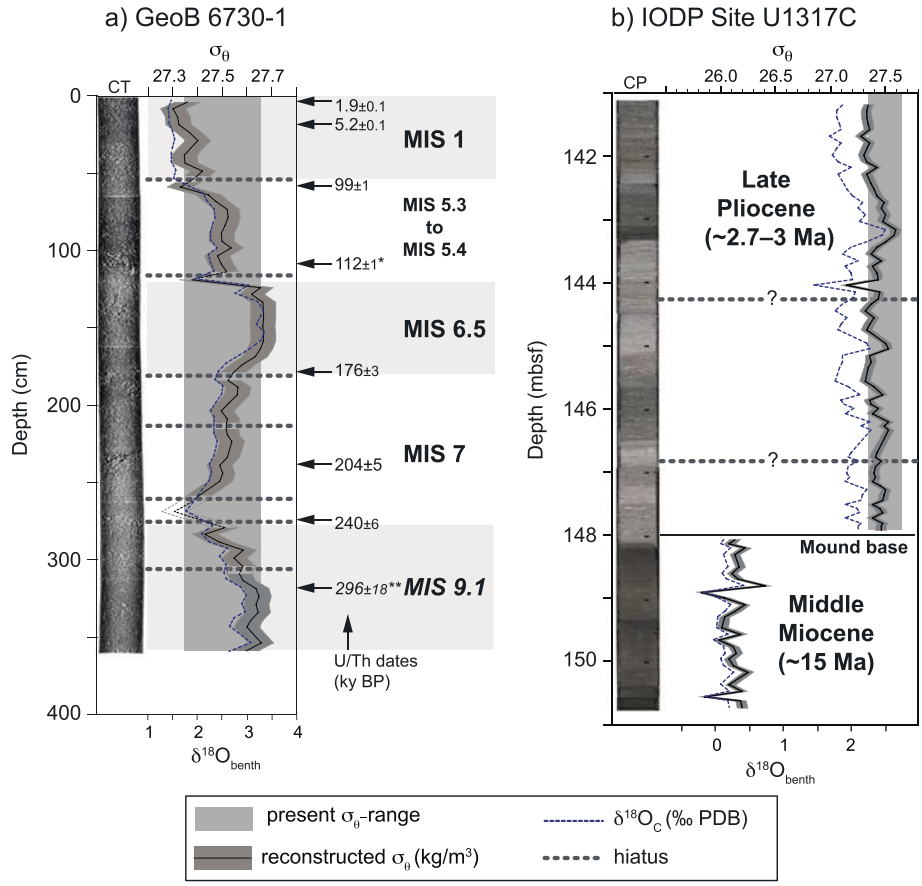

Figure 4. (a) Downcore record of core GeoB6730-1 of the past ~300 kyr for Propeller Mound. U/Th age data are in thousand years before present (kyr B.P.); corresponding Marine Isotope Stages (MIS) are indicated. The vertical gray bar highlights the present-day density range of $\sigma_\Theta = 27.35–27.65$ kg m^{-3} for living cold-water corals reefs of the NE Atlantic [*Dullo et al.*, 2008]. Reconstructed paleoseawater densities are shown by black line; dark grey envelope indicates the error bar. Computer tomographic (CT) images indicate occurrence of corals throughout the core with varying densities. An asterisk denotes mean value of three age determinations (see Table S1), and two asterisks denote large error comprising MIS 8.3 to MIS 9.2 (see supporting information). (b) Sedimentary record of IODP Site U1317C between 151 m and 141 m below the seafloor (mbsf). The vertical grey bar corresponds to the present-day density envelope. Stable oxygen isotopes and reconstructed σ_Θ values show a pronounced shift from middle Miocene to the onset of mound growth at ~2.7 Ma. Core pictures (CP) indicate the transition of dark grey, clayey sediments of the middle Miocene to the light grey, coral-bearing sediments of the late Pliocene with varying coral densities.

density range of $\sigma_\theta = 27.5 \pm 0.2$ kg m^{-3} also controls the development of CWC reefs and contemporaneously of the carbonate mounds during the past ~300 kyr. All paleodensity values of reef buildup phases recorded in core GeoB 6730-1 plot within or close to the modern density range of prolific CWC reef growth, with the Holocene (MIS 1) at the lighter ("warmer, more saline") margin and MIS 6.5 and MIS 9.1 at the heavier ("colder, fresher") one (Figure 5).

3.2. Cold-Water Coral Reef Development at the Begin of the Northern Hemisphere Glaciation

At the base of Challenger Mound we investigated 10 m of IODP core U1317C representing the transition from the glauconitic siltstones of the middle Miocene to the coral-bearing, unlithified, mixed siliciclastic/pelagic-carbonate sediments [*Ferdelman et al.*, 2006] indicating the onset of CWC reef growth at ~2.7 Ma [*Kano et al.*, 2007; *Raddatz et al.*, 2014] (Figure 4b). For the late Pliocene-early Pleistocene sediments of U1317C mean $\delta^{18}O_C$ values of 2.0 ± 0.18‰ correspond to the early interglacial periods (Figure 4b and Table S5). The range of these values is mainly at the lighter part of the intermediate setting (1.9–3.2‰); therefore, we applied equation (7) to reconstruct paleo-densities for the early CWC reef growth. For comparative reasons we applied the same equation (7) for the data

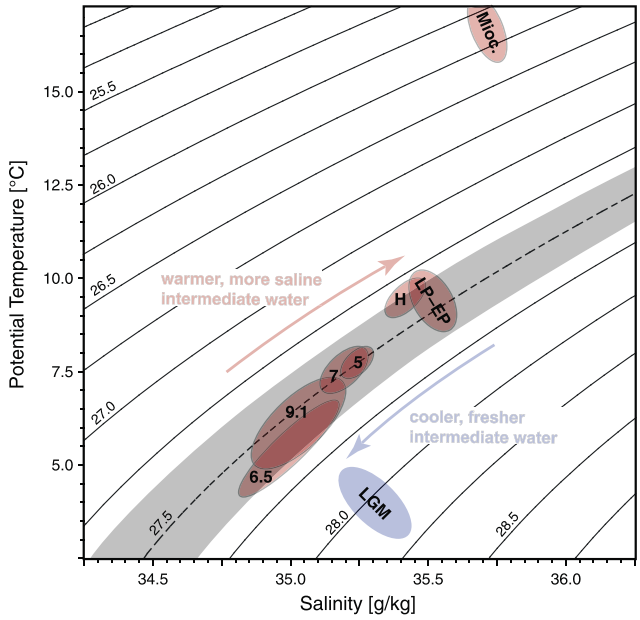

Figure 5. Potential temperature and salinity plot including pycnoclines of potential seawater density (σ_Θ in kg m^{-3}). Grey band corresponds to the present-day potential density range of CWC reefs along the European continental margin. Paleodensities derived for the middle Miocene before mound initiation are much lighter than the late Pliocene-Pleistocene-Holocene reconstructions. Paleotemperatures for the Miocene are from *Raddatz et al.* [2011] and *Khélifi et al.* [2009]. The onset of mound growth at ~3–2.7 Ma (late Pliocene-early Pleistocene, LP-EP) and the Holocene (H) plot at the lighter end of the present-day density range (27.3–27.6 kg m^{-3}). MIS 5 (= 5.3–5.4) and MIS 7 are directly on the isopycnal of 27.5 kg m^{-3}, while MIS 6.5 and MIS 9.1 show the tendency to heavier values (27.4–27.7 kg m^{-3}). They exhibit cooler temperatures (Tables S4 and S5 in the supporting information) equivalent to modern cold-water coral reefs of northern Norway [*Dullo et al.*, 2008; *Rüggeberg et al.*, 2011]. The Last Glacial Maximum (LGM) reconstruction plots around 28 kg m^{-3} at temperatures below 5°C. For these temperatures the accuracy becomes increasingly larger (see section 2).

below the mound base, although mean $\delta^{18}O_C$ values of 0.12 ± 0.12‰ refer to a completely different setting during the middle Miocene.

After the long hiatus cold-water corals started to build-up Challenger Mound closely related to major changes in Pliocene-Pleistocene paleoceanography [*Kano et al.*, 2007]. The dramatic increase of 1.8‰ in $\delta^{18}O_C$ at the mound base indicates the mound initiation and corresponds to a shift of ~1.3 kg m^{-3} from lighter seawater densities for the middle Miocene (26.11 ± 0.12 kg m^{-3}) to late Pliocene-early Pleistocene values of 27.41 ± 0.08 kg m^{-3} (Figure 4b) applying the same equation. The late Pliocene-early Pleistocene paleoseawater density record is comparable to the late Pleistocene record of Propeller Mound showing values of 27.27–27.60 kg m^{-3} (Figure 4). Taking reconstructed temperatures of *Raddatz et al.* [2014] into account the Pliocene-Pleistocene values plot close to the Holocene values of core GeoB6730-1 (Figure 5).

Khélifi et al. [2014] reconstructed MOW flow patterns along the European continental margin between 2.5 and 3.7 Ma using among other proxies also $\delta^{18}O_C$ and Mg/Ca temperatures to derive paleoseawater densities. Their values are slightly heavier (between 28 and 29 kg m^{-3}) from drill cores situated 400 m deeper than Challenger Mound, but also fluctuations to $<$27.5 kg/m^3 occur at ~2.8 Ma. Using their benthic $\delta^{18}O_C$ data for DSDP Site 548 (1200 m water depth) at ~2.8 Ma of 3 to 4‰, bottom water densities of 27.7 to 28.2 kg m^{-3} can be determined using equation (7), comparable values as of *Khélifi et al.* [2014]. The variability of reconstructed bottom water densities at Challenger Mound (IODP Site U1317C) can be directly linked to fluctuations of intermediate water masses of the early MOW and other North Atlantic Central Water masses (e.g., ENAW; Figure 1). The early CWC reefs started to develop and actively buildup Challenger Mound, when the intermediate water mass setting developed a pycnocline with associated mechanisms (horizontal currents transporting nutrition and possible disperse coral larvae) as described by *Dullo et al.* [2008] or *White and Dorschel* [2010]. This intermediate water mass setting has been hypothesized by different studies [e.g., *De Mol et al.*, 2002; *Sakai et al.*, 2009; *Li et al.*, 2011; *Raddatz et al.*, 2014] but not proven by reconstructed bottom water parameters or seawater densities so far. Furthermore, this hydrographic setting controlled by the MOW outflow dynamics may have accounted for the whole Porcupine Seabight as all mounds root on the same unconformity [*De Mol et al.*, 2002] and were under the influence of same water masses upstream or downstream.

3.3. Critical Assessment of Paleodensity Reconstructions

The determination of paleoseawater densities based on benthic $\delta^{18}O_C$ using the method developed by *Lynch-Stieglitz et al.* [1999b] allows the reconstruction with a smaller uncertainty compared to other methods

[e.g., *Khélifi et al*., 2014]. However, a regional calibration is necessary due to the influence of different water masses and therefore different $\delta^{18}O_{SW}$-salinity characteristics, but also a temporal calibration is necessary, as intermediate water masses and their flow paths are climatically controlled and variable through time. We provide regional calibrated equations for three different hydrographic settings for the NE Atlantic, with peak interglacial, peak glacial, and intermediate settings (Figures 2 and 3). The use of intermediate equation (7), which almost corresponds to the Global Open Ocean calibration or its modifications with 4‰ higher fresh end-member of *Lynch-Stieglitz et al*. [1999b], gives quite a good estimate of Plio-Pleistocene bottom water densities for the NE Atlantic (Figure 3b). Approaching the extreme warm or cold climates requires the use of equation (3) (for $\delta^{18}O_C < 1.8‰$) or equation (6) (for $\delta^{18}O_C > 3‰$) for interglacial or glacial conditions, respectively. Here the magnitude of error may increase defining the point where to switch the equations as indicated by the vertical dotted lines at ~1.8 and 3‰ in Figure 3b.

Figure 5 also indicates reconstructed middle Miocene bottom water densities using equation (7). Based on calculated intermediate water temperatures of ~15°C for Challenger Mound [*Raddatz et al*., 2011] calculated seawater densities refer to salinities of 35.6 to 35.8 g kg^{-1} (Figure 5). This would be in agreement with earlier studies stating that warm and saline intermediate waters of southern origin prevailed during the Miocene Climatic Optimum [*Flower and Kennett*, 1994; *Wright et al*., 1992], although a recent study using an ocean circulation carbon cycle model of intermediate complexity shows a distinct freshening of 0.5 to 1 g kg^{-1} for the upper 1000 m of the middle Miocene NE Atlantic [*Butzin et al*., 2011]. Further studies on differently derived seawater salinity proxies, such as Na/Ca [*Wit et al*., 2013], for different hydrographic settings and for Pleistocene to Miocene times may strengthen the accuracy of our reconstructions. However, the advantage of the method applied here is that estimations of paleosalinities are possible using paleotemperatures and paleodensities plotted in the temperature-salinity plot including isopycnals (Figure 5).

4. Conclusion

Seawater densities of the past 3 Myr in the Porcupine Seabight (NE Atlantic) were reconstructed following the method introduced by *Lynch-Stieglitz et al*. [1999b] but using a regional calibration for three different climatic settings: (1) peak interglacial, (2) peak glacial, and (3) *intermediate setting*. The use of this method provides a relatively small uncertainty of ~0.1–0.15 kg m^{-3} of reconstructed seawater densities; however, it is regionally limited and a temporal accuracy is necessary.

The investigated sediment cores (GeoB6730-1, IODP Expedition 307 Site U1317C) retrieved from cold-water coral (CWC) carbonate mounds represent distinct intervals of CWC reef growth and carbonate mound development. The reconstructed seawater density values of these intervals vary from 27.2 to 27.7 kg m^{-3} and coincide with the modern seawater density range (27.5 ± 0.15 kg m^{-3}) in which prolific CWC reefs occur along the European continental margin.

These results imply that comparable conditions like today with a pycnocline at intermediate water depths occurred during CWC carbonate mound initiation and later development. On this pycnocline internal waves can propagate and horizontal currents can develop [*White*, 2007; *Pomar et al*., 2012] which are fundamental mechanisms for transporting nutrition and possible dispersal of coral larvae [*Dullo et al*., 2008; *Mazzini et al*., 2012; *Pomar et al*., 2012].

This study demonstrates that CWC reef formation and carbonate mound development in the NE Atlantic is triggered by processes and dynamics of ocean gateways: (1) Mediterranean Outflow at the Strait of Gibraltar intensified 3.3–3.5 Ma leading to a gradual increase of bottom water densities [*Hernández-Molina et al*., 2014] and (2) the closure of the Isthmus of Panama around 2.7 Ma [*Haug and Tiedemann*, 1998] or at least the onset of the meridional overturning circulation resulted in an enhanced subsurface water transport to higher latitudes in the Atlantic lowering the extinction risk of deep-sea ecosystems [*Henry et al*., 2014]. The consequences of the gateway processes established the necessary density contrast in water masses enabling active CWC reef growth in the Porcupine Seabight around that time [*Foubert and Henriet*, 2009; *Raddatz et al*., 2011].

Overall, CWC carbonate mound growth portrays prolific marine benthic ecosystem development and is linked to small changes in ambient bottom water characteristics (i.e., density). These results show that marine benthic ecosystems occupy very narrow and specific ecological niches, which are very sensitive and even at

risk to the actual global environmental changes, such as bottom water warming and acidification. As a consequence, our findings have lead to a robust diagnostic key tool for the interpretation of basin-wide sudden onset or shutdown of carbonate mound growth during Earth history [e.g., *Wood*, 1999].

Acknowledgments
We thank captains, crews, and shipboard scientific parties of R/V *Poseidon* cruise P265 and of R/V *Joides* Resolution IODP Expedition 307. The study received funding from the Deutsche Forschungsgemeinschaft (DFG) projects TRISTAN, ISOLDE, and INWADE (Du 129/37, Du 129/45, and Du 129/48). A.R. additionally received funding from FWO International Coordination Action COCARDE-ICA (G.0852-09.N), which he greatly acknowledges. This study is part of ESF Research Network Programme COCARDE-ERN, a European Research Network on carbonate mound research. Furthermore, we are indebted to Nils Andersen, Leibniz Laboratory at Kiel University, for conducting stable oxygen isotope measurements of water samples. Jan Fietzke is especially acknowledged for maintaining the Axiom MC-ICP-MS on high performance for the U-Th measurements and analytical collaboration. Folkmar Hauff is gratefully acknowledge for supporting the TIMS work, as well as Anna Kolevica for her clean-lab support, Jutta Heinze for XRD measurements on smallest sample amounts, and Lutz Haxhiaj for performing C and O isotope measurements on the carbonate samples (all GEOMAR). Anton Eisenhauer is thanked for providing the MS facilities at GEOMAR. The journal Editor Christopher Charles and an anonymous reviewer are thanked for their valuable comments, which improved the manuscript considerably. We are indebted to the A.P. Laudenbacher Foundation in La Punt Chamues-ch providing an excellent atmosphere for a working and research retreat. Supporting data are included as six tables and three figures in a supporting information file. All other data for this paper are properly cited and referred to in the reference list.

References

Beuck, L., and A. Freiwald (2005), Bioerosion patterns in a deep-water *Lophelia pertusa* (Scleractinia) thicket (Propeller Mound, northern Porcupine Seabight), in *Cold-Water Corals and Ecosystems*, edited by A. Freiwald and J. M. Roberts, pp. 915–936, Springer, Berlin.

Blanchon, P., A. Eisenhauer, J. Fietzke, and V. Liebetrau (2009), Rapid sea-level rise and reef back-stepping at the close of the last interglacial highstand, *Nature*, *458*, 881–885.

Braconnot, P., et al. (2007), Results of PMIP2 coupled simulations of the Mid-Holocene and last glacial maximum—Part 1: Experiments and large-scale features, *Clim. Past*, *3*, 261–277.

Butzin, M., G. Lohmann, and T. Bickert (2011), Miocene ocean circulation inferred from marine carbon cycle modeling combined with benthic isotope records, *Paleoceanography*, *26*, PA1203, doi:10.1029/2009PA001901.

Cheng, H., J. Adkins, R. L. Edwards, and E. A. Boyle (2000a), U-Th dating of deep-sea corals, *Geochim. Cosmochim. Acta*, *64*(14), 2401–2416.

Cheng, H., R. L. Edwards, J. Hoff, C. D. Gallup, D. A. Richards, and Y. Asmerom (2000b), The half-lives of Uranium-234 and Thorium-230, *Chem. Geol.*, *169*(1–2), 17–33.

Davies, A. J., M. Wisshak, J. C. Orr, and J. M. Roberts (2008), Predicting suitable habitat for the cold-water coral *Lophelia pertusa* (Scleractinia), *Deep Sea Res., Part I*, *55*, 1048–1062.

de Haas, H., F. Mienis, N. Frank, T. Richter, R. Steinacher, H. C. de Stigter, C. van der Land, and T. C. E. van Weering (2009), Morphology and sedimentology of (clustered) cold-water coral mounds at the south Rockall Trough margins, NE Atlantic Ocean, *Facies*, *55*, 1–26.

De Mol, B., P. Van Rensbergen, S. Pillen, K. Van Herreweghe, D. Van Rooij, A. McDonnell, V. Huvenne, M. Ivanov, R. Swennen, and J. P. Henriet (2002), Large deep-water coral banks in the Porcupine Basin, southwest of Ireland, *Mar. Geol.*, *188*, 193–231.

De Mol, B., J.-P. Henriet, and M. Canals (2005), Development of coral banks in Porcupine Seabight: Do they have Mediterranean ancestors? in *Cold-Water Corals and Ecosystems*, edited by A. Freiwald and J. M. Roberts, pp. 515–533, Springer, Berlin.

De Mol, L., D. Van Rooij, H. Pirlet, J. Greinert, N. Frank, F. Quemmerais, and J.-P. Henriet (2011), Cold-water coral habitats in the Penmarc'h and Guilvinec Canyons (Bay of Biscay): Deep-water versus shallow-water settings, *Mar. Geol.*, *282*, 40–52.

Dickson, R. R., and I. N. McCave (1986), Nepheloid layers on the continental slope west of Porcupine Bank, *Deep Sea Res., Part A*, *33*(6), 791–818.

Dokken, T. M., and E. Jansen (1999), Rapid changes in the mechanism of ocean convection during the last glacial period, *Nature*, *401*, 458–461.

Dorschel, B., D. Hebbeln, A. Rüggeberg, W.-C. Dullo, and A. Freiwald (2005), Growth and erosion of a cold-water coral covered carbonate mound in the northeast Atlantic during the late Pleistocene and Holocene, *Earth Planet. Sci. Lett.*, *233*, 33–44.

Dorschel, B., D. Hebbeln, A. Foubert, M. White, and A. J. Wheeler (2007), Hydrodynamics and cold-water coral facies distribution related to recent sedimentary processes at Galway Mound west of Ireland, *Mar. Geol.*, *244*, 184–195.

Dorschel, B., A. J. Wheeler, X. Monteys, and K. Verbruggen (2010), *Atlas of the Deep-Water Seabed: Ireland*, Springer, Dordrecht, Netherlands.

Dullo, W.-C., S. Flögel, and A. Rüggeberg (2008), Cold-water coral growth in relation to the hydrography of the Celtic and Nordic European continental margin, *Mar. Ecol. Prog. Ser.*, *371*, 165–176.

Edwards, R. L., J. H. Chen, and G. J. Wasserburg (1986), ^{238}U–^{234}U–^{230}Th–^{232}Th systematics and the precise measurement of time over the past 500,000 years, *Earth Planet. Sci. Lett.*, *81*, 175–192.

Eisele, M., D. Hebbeln, and C. Wienberg (2008), Growth history of a cold-water coral covered carbonate mound—Galway Mound, Porcupine Seabight, NE-Atlantic, *Mar. Geol.*, *253*, 160–169.

Eisele, M., N. Frank, C. Wienberg, D. Hebbeln, M. López Correa, E. Douville, and A. Freiwald (2011), Productivity controlled cold-water coral growth periods during the last glacial off Mauritania, *Mar. Geol.*, *280*, 143–149.

European Commission (2007), *The Deep-Sea Frontier: Science Challenges for a Sustainable Future*, *EUR 22812 EN*, 53 pp., Off. for Off. Publ. of the Eur. Communities, Luxembourg.

Ferdelman, T. G., A. Kano, T. Williams, and the IODP Expedition 307 Scientists (2006), IODP Expedition 307 drills cold-water coral mound along the Irish continental margin, *Sci. Drill.*, *2*, 11–16, doi:10.2204/iodp.sd.2.02.2006.

Fietzke, J., V. Liebetrau, A. Eisenhauer, and C. Dullo (2005), Determination of uranium isotope ratios by multi-static MIC-ICP-MS: Method and implementation for precise U- and Th-series isotope measurements, *J. Anal. At. Spectrom.*, *20*, 1–7.

Flögel, S., W.-C. Dullo, O. Pfannkuche, K. Kiriakoulakis, and A. Rüggeberg (2014), Geochemical and physical constraints for the occurrence of living cold-water corals, *Deep Sea Res., Part II*, *99*, 19–26.

Flower, B. P., and J. P. Kennett (1994), The middle Miocene climatic transition: East Antarctic ice sheet development, deep ocean circulation and global carbon cycling, *Palaeogeogr. Palaeoclimatol. Palaeoecol.*, *108*, 537–555.

Form, A., and U. Riebesell (2012), Acclimation to ocean acidification during long-term CO_2 exposure in the cold-water coral *Lophelia pertusa*, *Global Change Biol.*, *18*(3), 843–853.

Foubert, A., and J.-P. Henriet (2009), *Nature and Significance of the Recent Carbonate Mound Record*, 298 pp., Springer, Berlin.

Foubert, A., T. Beck, A. J. Wheeler, J. Opderbecke, A. Grehan, M. Klages, J. Thiede, J.-P. Henriet, and the Polarstern ARK-XIX/3a Shipboard Party (2005), New view of the Belgica Mounds, Porcupine Seabight, NE Atlantic: Preliminary results from the Polarstern ARK-XIX/3a ROV cruise, in *Cold-Water Corals and Ecosystems*, edited by A. Freiwald and J. M. Roberts, pp. 403–415, Springer, Berlin.

Frank, N., M. Paterne, L. Ayliffe, T. van Weering, J.-P. Henriet, and D. Blamart (2004), Eastern North Atlantic deep-sea corals: Tracing upper intermediate water Δ^{14}C during the Holocene, *Earth Planet. Sci. Lett.*, *219*, 297–309.

Frank, N., et al. (2011), Northeastern Atlantic cold-water coral reefs and climate, *Geology*, *39*(8), 743–746.

Freiwald, A. (2002), Reef-forming cold-water corals, in *Ocean Margin Systems*, edited by G. Wefer et al., pp. 365–385 , Springer, Berlin.

Freiwald, A., J. H. Fosså, A. Grehan, T. Koslow, and J. M. Roberts (2004), *Cold-Water Coral Reefs*, 84 pp., UNEO-WCMC, Cambridge, U. K.

Haug, G. H., and R. Tiedemann (1998), Effect of the formation of the Isthmus of Panama on Atlantic Ocean thermohaline circulation, *Nature*, *393*, 673–676.

Hebbeln, D., et al. (2014), Environmental forcing of the Campeche cold-water coral province, southern Gulf of Mexico, *Biogeosciences*, *11*, 1799–1815.

Heindel, K., J. Titschack, B. Dorschel, V. A. I. Huvenne, and A. Freiwald (2010), The sediment composition and predictive mapping of facies on the Propeller Mound—A cold-water coral mound (Porcupine Seabight, NE Atlantic), *Cont. Shelf Res.*, *30*, 1814–1829.

Henderson, G. M., and R. F. Anderson (2003), The U-series toolbox for paleoceanography, *Rev. Mineral. Geochem.*, *52*, 493–531.
Henriet, J. P., et al. (1998), Gas hydrate crystals may help build reefs, *Nature*, *391*, 648–649.
Henry, L.-A., et al. (2014), Global ocean conveyor lowers extinction risk in the deep sea, *Deep Sea Res., Part I*, *88*, 8–16.
Hernández-Molina, F. J., et al. (2014), Onset of Mediterranean outflow into the North Atlantic, *Science*, *344*(6189), 1244–1250.
Hübscher, C., C. Dullo, S. Flögel, J. Titschack, and J. Schönfeld (2010), Contourite drift evolution and related coral growth in the eastern Gulf of Mexico and its gateways, *Int. J. Earth Sci.*, *99*, S191–S206.
Intergovernmental Panel on Climate Change (2014), *Climate Change 2014: Synthesis Report. Contribution of Working Groups I, II and III to the Fifth Assessment Report of the Intergovernmental Panel on Climate Change*, edited by Core Writing Team, R. K. Pachauri, and L. A. Meyer, 151 pp., IPCC, Geneva, Switzerland.
Kano, A., et al. (2007), Age constraints on the origin and growth history of a deep-water coral mound in the northeast Atlantic drilled during Integrated Ocean Drilling Program Expedition 307, *Geology*, *35*(11), 1051–1054.
Khélifi, N., M. Sarnthein, N. Andersen, T. Blanz, M. Frank, D. Garbe-Schönberg, B. A. Haley, R. Stumpf, and M. Weinelt (2009), A major and long-term Pliocene intensification of the Mediterranean outflow, 3.5–3.3 Ma ago, *Geology*, *37*(9), 811–814.
Khélifi, N., M. Sarnthein, M. Frank, N. Andersen, and D. Garbe-Schönberg (2014), Late Pliocene variations of the Mediterranean outflow, *Mar. Geol.*, *357*, 182–194.
Li, X., C. Takashima, A. Kano, S. Sakai, Y. Chen, B. Xu, and I. E. Scientists (2011), Pleistocene geochemical stratigraphy of the borehole 1317E (IODP Expedition 307) in Porcupine Seabight, SW of Ireland: Applications to palaeoceanography and palaeoclimate of the coral mound development, *J. Quat. Sci.*, *26*(2), 178–189.
Liebetrau, V., A. Eisenhauer, and P. Linke (2010), Cold seep carbonates and associated cold-water corals at the Hikurangi Margin, New Zealand: New insights into fluid pathways, growth structures and geochronology, *Mar. Geol.*, *272*, 307–318.
Lisiecki, L. E., and M. E. Raymo (2005), A Pliocene-Pleistocene stack of 57 globally distributed benthic $\delta^{18}O$ records, *Paleoceanography*, *20*, PA1003, doi:10.1029/2004PA001071.
Lisiecki, L. E., and M. E. Raymo (2007), Plio-Pleistocene climate evolution: Trends and transitions in glacial cycle dynamics, *Quat. Sci. Rev.*, *26*, 56–69.
López Correa, M., P. Montagna, N. Joseph, A. Rüggeberg, J. Fietzke, S. Flögel, B. Dorschel, S. L. Goldstein, A. Wheeler, and A. Freiwald (2012), Preboreal onset of cold-water coral growth beyond the Arctic circle revealed by coupled radiocarbon and U-series dating and neodymium isotopes, *Quat. Sci. Rev.*, *34*, 24–43.
Lutringer, A., D. Blamart, N. Frank, and L. Labeyrie (2005), Paleotemperatures from deep-sea corals: Scale effects, in *Cold-Water Corals and Ecosystems*, edited by A. Freiwald and J. M. Roberts, pp. 1081–1096, Springer, Berlin.
Lynch-Stieglitz, J., W. B. Curry, and N. Slowey (1999a), Weaker gulf stream in the Florida Straits during the last glacial maximum, *Nature*, *402*, 644–648.
Lynch-Stieglitz, J., W. B. Curry, and N. Slowey (1999b), A geostrophic transport estimate for the Florida current from the oxygen isotope composition of benthic foraminifera, *Paleoceanography*, *14*, 360–373.
Maier, C., P. Watremez, M. Taviani, M. G. Weinbauer, and J. P. Gattuso (2011), Calcification rates and the effect of ocean acidification on Mediterranean cold-water corals, *Proc. R. Soc. B*, *276*, 1716–1723, doi:10.1098/rspb.2011.1763.
Marchitto, T. M., W. B. Curry, J. Lynch-Stieglitz, S. P. Bryan, K. M. Cobb, and D. C. Lund (2014), Improved oxygen isotope temperature calibrations for cosmopolitan benthic foraminifera, *Geochim. Cosmochim. Acta*, *130*, 1–11.
Mazzini, A., A. Akhmetzhanov, X. Monteys, and M. Ivanov (2012), The Porcupine Bank Canyon coral mounds: Oceanographic and topographic steering of deep-water carbonate mound development and associated phosphatic deposition, *Geo Mar. Lett.*, *32*, 205–225.
McCulloch, M., M. Taviani, P. Montagna, M. López Correa, A. Remia, and G. Mortimer (2010), Proliferation and demise of deep-sea corals in the Mediterranean during the Younger Dryas, *Earth Planet. Sci. Lett.*, *298*, 143–152.
Mienis, F., C. van der Land, H. C. de Stigter, M. van de Vorstenbosch, H. de Haas, T. Richter, and T. C. E. van Weering (2009), Sediment accumulation on a cold-water carbonate mound at the Southwest Rockall Trough margin, *Mar. Geol.*, *265*, 40–50.
Oppo, D. W., J. F. McManus, and J. L. Cullen (2006), Evolution and demise of the Last Interglacial warmth in the subpolar North Atlantic, *Quat. Sci. Rev.*, *25*(23–24), 3268–3277.
Peacock, S., E. Lane, and J. M. Restrepo (2006), A possible sequence of events for the generalized glacial-interglacial cycle, *Global Biogeochem. Cycles*, *20*, GB2010, doi:10.1029/2005GB002448.
Peck, V. L., I. R. Hall, R. Zahn, H. Elderfield, F. Grousset, S. R. Hemming, and J. D. Scourse (2006), High resolution evidence for linkages between NW European ice sheet instability and Atlantic meridional overturning circulation, *Earth Planet. Sci. Lett.*, *243*, 476–488.
Pomar, L., M. Morsilli, P. Hallock, and B. Bádenas (2012), Internal waves, an under-explored source of turbulence events in the sedimentary record, *Earth Sci. Rev.*, *111*, 56–81.
Raddatz, J., A. Rüggeberg, S. Margreth, W.-C. Dullo, and IODP Expedition 307 Scientific Party (2011), Paleoenvironmental reconstruction of Challenger Mound initiation in the Porcupine Seabight, NE Atlantic, *Mar. Geol.*, *282*, 79–90.
Raddatz, J., A. Rüggeberg, V. Liebetrau, A. Foubert, E. C. Hathorne, J. Fietzke, A. Eisenhauer, and W.-C. Dullo (2014), Environmental boundary conditions of cold-water coral mound growth over the last 3 million years in the Porcupine Seabight, Northeast Atlantic, *Deep Sea Res., Part II*, *99*, 227–236.
Rice, A. L., D. S. M. Billett, M. H. Thurston, and R. S. Lampitt (1991), The institute of oceanographic sciences biology programme in the Porcupine Seabight: Background and general introduction, *J. Mar. Biol.*, *71*, 281–310.
Roberts, J. M., A. J. Wheeler, and A. Freiwald (2006), Reefs of the deep: The biology and geology of cold-water coral ecosystem, *Science*, *312*, 543–547.
Robinson, L. F., N. S. Belshaw, and G. M. Henderson (2004), U and Th concentrations and isotope ratios in modern carbonates and waters from the Bahamas, *Geochim. Cosmochim. Acta*, *68*(8), 1777–1789.
Robinson, L. F., J. F. Adkins, D. S. Scheirer, D. P. Fernandez, A. Gagnon, and R. G. Waller (2007), Deep-sea scleractinian coral age and depth distributions in the northwest Atlantic for the last 225,000 years, *Bull. Mar. Sci.*, *81*(3), 371–391.
Rüggeberg, A., B. Dorschel, W.-C. Dullo, and D. Hebbeln (2005), Sedimentary patterns in the vicinity of a carbonate mound in the Hovland Mound province, northern Porcupine Seabight, in *Cold-Water Corals and Ecosystems*, edited by A. Freiwald and J. M. Roberts, pp. 87–112, Springer, Berlin.
Rüggeberg, A., C. Dullo, B. Dorschel, and D. Hebbeln (2007), Environmental changes and growth history of Propeller Mound, Porcupine Seabight: Evidence from benthic foraminiferal assemblages, *Int. J. Earth Sci.*, *96*, 57–72.
Rüggeberg, A., S. Flögel, W.-C. Dullo, K. Hissmann, and A. Freiwald (2011), Water mass characteristics and sill dynamics in a subpolar cold-water coral reef setting at Stjernsund, northern Norway, *Mar. Geol.*, *282*, 5–12.
Sakai, S., A. Kano, and K. Abe (2009), Origin, glacial-interglacial responses, and controlling factors of a cold-water coral mound in NE Atlantic, *Paleoceanography*, *24*, PA2213, doi:10.1029/2008PA001695.
Sánchez, F., et al. (2014), Habitat characterization of deep-water coral reefs in La Gaviera Canyon (Avilés Canyon System, Cantabrian Sea), *Deep Sea Res., Part II*, *106*, 118–140.

Schmidt, G. A., G. R. Bigg, and E. J. Rohling (1999), Global seawater oxygen-18 database. [Available at http://data.giss.nasa.gov/o18data/].
Schönfeld, J., W.-C. Dullo, O. Pfannkuche, A. Freiwald, A. Rüggeberg, S. Schmidt, and J. Weston (2011), Recent benthic foraminiferal assemblages from cold-water coral mounds in the Porcupine Seabight, *Facies*, *57*, 187–213.
Schrag, D. P., J. F. Adkins, K. McIntyre, J. L. Alexander, D. A. Hodell, C. D. Charles, and J. F. McManus (2002), The oxygen isotopic composition of seawater during the Last Glacial Maximum, *Quat. Sci. Rev.*, *21*, 331–342.
Somoza, L., G. Ercilla, V. Urgorri, R. León, T. Medialdea, M. Paredes, F. J. Gonzalez, and M. A. Nombela (2014), Detection and mapping of cold-water coral mounds and living *Lophelia* reefs in the Galicia Bank, Atlantic NW Iberia margin, *Mar. Geol.*, *349*, 73–90.
Thiagarajan, N., D. Gerlach, M. L. Roberts, A. Burke, A. McNichol, W. J. Jenkins, A. V. Subhas, R. E. Thresher, and J. F. Adkins (2013), Movement of deep-sea coral populations on climatic timescales, *Paleoceanography*, *28*, 227–236, doi:10.1002/palo.20023.
Thierens, M., J. Titschack, B. Dorschel, V. A. I. Huvenne, A. J. Wheeler, J.-B. Stuut, and R. O'Donnell (2010), The 2.6 Ma depositional sequence from the Challenger cold-water coral carbonate mound (IODP Exp. 307): Sediment contributors and hydrodynamic palaeo-environments, *Mar. Geol.*, *271*, 260–277.
Thierens, M., E. Browning, H. Pirlet, M.-F. Loutre, B. Dorschel, V. A. I. Huvenne, J. Titschack, C. Colin, A. Foubert, and A. J. Wheeler (2013), Cold-water coral carbonate mounds as unique palaeo-archives: The Plio-Pleistocene Challenger Mound record (NE Atlantic), *Quat. Sci. Rev.*, *73*, 14–30.
Thompson, W. G., M. W. Spiegelman, S. L. Goldstein, and R. C. Speed (2003), An open-system model for U-series age determinations of fossil corals, *Earth Planet. Sci. Lett.*, *210*, 365–381.
Titschack, J., M. Thierens, B. Dorschel, C. Schulbert, A. Freiwald, A. Kano, C. Takashima, N. Kawagoe, X. Li, and IODP Expedition 307 Scientific Party (2009), Carbonate budget of a cold-water coral mound (Challenger Mound, IODP Exp. 307), *Mar. Geol.*, *259*, 36–46.
Venz, K. A., D. A. Hodell, C. Stanton, and D. A. Warnke (1999), A 1.0 Myr record of glacial North Atlantic intermediate water variability from OPD site 982 in the northeast Atlantic, *Paleoceanography*, *14*, 42–52.
Wedepohl, K. H. (1995), The composition of the continental crust, *Geochim. Cosmochim. Acta*, *59*(7), 1217–1232.
White, M. (2007), Benthic dynamics at the carbonate mound regions of the Porcupine Sea Bight continental margin, *Int. J. Earth Sci.*, *97*, 1–9.
White, M., and B. Dorschel (2010), The importance of the permanent thermocline to the cold water coral carbonate mound distribution in the NE Atlantic, *Earth Planet. Sci. Lett.*, *296*, 395–402.
Wienberg, C., N. Frank, K. N. Mertens, J.-S. Stuut, M. Marchant, J. Fietzke, F. Mienis, and D. Hebbeln (2010), Glacial cold-water coral growth in the Gulf of Cádiz: Implications of increased palaeo-productivity, *Earth Planet. Sci. Lett.*, *298*, 405–416.
Williams, T., et al. (2006), Cold-water coral mounds revealed, *Eos Trans. AGU*, *87*(47), 525–536.
Wit, J. C., L. J. de Nooijer, M. Wolthers, and G. J. Reichart (2013), A novel salinity proxy based on Na incorporation into foraminiferal calcite, *Biogeosciences*, *10*, 6375–6387.
Wood, R. (1999), *Reef Evolution*, 414 pp., Oxford Univ. Press, Oxford, U. K.
Wright, J. D., K. G. Miller, and R. Fairbanks (1992), Early and Middle Miocene stable isotopes: Implication for deepwater circulation and climate, *Paleoceanography*, *7*, 357–389.